

# Neutron matter within QCD sum rules

Bao-Jun Cai<sup>1,2</sup> and Lie-Wen Chen<sup>\*2,3</sup>

<sup>1</sup>*Department of Physics, Shanghai University, Shanghai 200444, China*

<sup>2</sup>*School of Physics and Astronomy and Shanghai Key Laboratory for Particle Physics and Cosmology, Shanghai Jiao Tong University, Shanghai 200240, China*

<sup>3</sup>*Center of Theoretical Nuclear Physics, National Laboratory of Heavy Ion Accelerator, Lanzhou 730000, China*  
(Dated: April 10, 2022)

Equation of state (EOS) of pure neutron matter (PNM) is studied in QCD sum rules (QCDSR). It is found that the QCDSR results on EOS of PNM are in good agreement with predictions by current advanced microscopic many-body theories. Moreover, the higher-order density terms in quark condensates are shown to be important to describe the empirical EOS of PNM in the density region around and above nuclear saturation density although they play minor role at subsaturation densities. The chiral condensates in PNM are also studied, and our results indicate that the higher-order density terms in quark condensates, which are introduced to reasonably describe the empirical EOS of PNM at suprasaturation densities, tend to hinder the appearance of chiral symmetry restoration in PNM at high densities.

PACS numbers: 21.65.Cd, 21.30.Fe, 12.38.Lg

## I. INTRODUCTION

Equation of state (EOS) of cold pure neutron matter (PNM) is an interesting and important problem at least from two aspects. On the one hand, at sub-saturation even to very low densities, the PNM composed of spin-down and -up neutrons with a large s-wave scattering length shows several universal properties [1] such as the simplicity of its EOS characterized by a few universal parameters [2–5]; the high momentum tail above the Fermi surface of the single nucleon momentum distribution function in cold PNM is also found to be very similar to that in ultra-cold atomic Fermi gases [6] although the magnitude of the density for the two systems differs by about 25 orders [7]. Thus, the cold PNM at low densities provides a perfect testing bed to explore novel ideas in the unitary region [8, 9], helping to find deep physical principles behind these quantum many-body systems [10]. On the other hand, cold PNM at densities up to  $3\text{--}5\rho_0$ , with  $\rho_0 \sim 0.16 \text{ fm}^{-3}$  the nuclear saturation density, is extremely important to the properties of neutron stars [11–15], such as the mass-radius relation of a neutron star and its transport properties [16], since the EOS of neutron star matter is very close to that of PNM.

Conventionally, since there lack direct experimental probes on the PNM [17], people usually rely on phenomenological models [18, 19] to explore its properties. However, due to the fact that the fitting scheme in these models is usually implemented by a number of phenomenological parameters, the microscopic origin of the uncertainties on the EOS of PNM are often averaged. Consequently, any microscopic approaches to EOS of PNM, especially those inheriting the quantum chromodynamics (QCD) spirit, such as the effective field theories [20–26] and simulations [27], are appealing and exciting.

The QCD sum rules (QCDSR) method [28] provides an important non-perturbative QCD approach to explore the properties of nuclear matter (see, e.g., Refs. [29]). Intuitively, when

the QCD coupling constant is small at high energies/small distances, the theory becomes asymptotically free, guaranteeing the applicability of perturbative calculations. As the energy scale decreases, the coupling constant of the theory becomes large, perturbative methods break down eventually and non-perturbative effects emerge. Among these effects, the most important is the appearance of the quark/gluon condensates. The basic idea of QCDSR for nuclear matter calculations [29–37] is to relate these condensates to the nucleon self-energies using the operator product expansion (OPE) technique, where information on the self-energies is introduced via nucleon-nucleon correlation functions. Within the QCDSR method, the exact information on the nucleon self-energies and nuclear matter EOS can thus provide constraints on the in-medium quark condensate, which is an order parameter of spontaneous chiral symmetry breaking in QCD. The QCDSR method is expected to work well at lower densities/momenta where effects of the poorly-known high mass-dimensional condensates as well as continuum effects are small enough.

In this work, we mainly focus on the properties of PNM obtained with the QCDSR, and leave the detailed descriptions and more physical issues about asymmetric nuclear matter to be reported elsewhere [38]. The EOS of PNM defined by the energy per neutron can be obtained as [39, 40]

$$E_n(\rho) = \frac{1}{\rho} \int_0^\rho d\rho [e_n^*(\rho) + \Sigma_V^n(\rho, k_F^n) - M], \quad (1)$$

where we denote  $e_n^*(\rho) = [(M + \Sigma_S^n(\rho, k_F^n))^2 + k_F^{n,2}]^{1/2}$  with  $M$  the nucleon rest mass, and  $\Sigma_{S/V}^n(\rho, k_F^n)$  is the scalar/vector self-energy of a neutron in PNM at its Fermi surface  $k_F^n = (3\pi^2\rho)^{1/3}$ . This Lorentz structure of the single neutron energy  $e_n = e_n^* + \Sigma_V^n$  is very general owing to the translational/rotational/parity and time-reversal invariance as well as the hermiticity in the rest frame of neutron matter [19, 41]. The main motivation of this work is to obtain the  $E_n(\rho)$  by Eq.(1) with the density and momentum dependent self-energies, i.e.,  $\Sigma_{S/V}^n(\rho, |\mathbf{k}|)$ , determined by the QCDSR.

Successes of QCDSR in nuclear matter calculations can be traced back to the prediction on the large nucleon self-energies

\*Corresponding author: lwchen@sjtu.edu.cn

on GeV scale [30]. And the present work is a natural generalization to the study of PNM with QCDSR. As we shall see, the results on EOS of PNM and quark condensates at low densities obtained via the QCDSR are consistent with predictions by other state-of-the-art microscopic many body theories, demonstrating that QCDSR can be applied to explore properties of PNM quantitatively.

Section II briefly introduces the QCDSR method. In section III, the results on the  $E_n(\rho)$  from the QCDSR are presented. Section IV is devoted to the study on the chiral condensates in PNM. Section V is the summary of this work.

## II. A BRIEF INTRODUCTION TO QCDSR

As discussed in the introduction, the essential task of the QCDSR calculations for nuclear matter is to relate, via OPE, the quark/gluon condensates with the nucleon self-energies, and the latter are usually encapsulated in the nucleon-nucleon correlation functions  $\Pi_{\mu\nu}$  constructed by quantum hadrodynamics [19]. The form of  $\Pi_{\mu\nu}$  at zero density (vacuum) is generally given by [33]

$$\begin{aligned} \Pi_{\mu\nu}(q) &\equiv i \int d^4x e^{iqx} \langle 0 | T \eta_\mu(x) \bar{\eta}_\nu(0) | 0 \rangle \\ &= - \int da_0 \left[ \frac{\rho_{\mu\nu}(a)}{q_0 - a_0 + i0^+} + \frac{\tilde{\rho}_{\mu\nu}(a)}{q_0 - a_0 - i0^+} \right], \quad (2) \end{aligned}$$

where  $q$  is the momentum transfer and  $a = (a_0, \mathbf{q})$ ,  $|0\rangle$  is the non-perturbative vacuum,  $\mu, \nu$  are the Dirac spinor indices. Moreover,  $\eta_\mu$  is the interpolation field of nucleons, and for the proton,  $\eta_p(x) = 2[t\eta_1^p(x) + \eta_2^p(x)]$ , where two independent terms are given by  $\eta_1^p(x) = \varepsilon_{abc} [u_a^T C \gamma_5 d_b(x)] u_c(x)$  and  $\eta_2^p(x) = \varepsilon_{abc} [u_a^T C d_b(x)] \gamma_5 u_c(x)$ , with  $C$  the charge conjugate operator, and  $t$  called the Ioffe parameter whose value is around  $-1$  [42]. In this work, the value of  $t$  is determined via the nucleon mass in vacuum [38]. In order to obtain the interpolation field for neutron, one can make the exchange “ $u \leftrightarrow d$ ”.

In Eq. (2),  $\rho_{\mu\nu} = (2\pi)^{-1} \int d^4x e^{iqx} \langle 0 | \eta_\mu(x) \bar{\eta}_\nu(0) | 0 \rangle$  and  $\tilde{\rho}_{\mu\nu} = (2\pi)^{-1} \int d^4x e^{iqx} \langle 0 | \bar{\eta}_\nu(0) \eta_\mu(x) | 0 \rangle$  are nucleon spectral densities. Moreover, Lorentz symmetry and parity invariance together indicate that the general structure of the spectral density is  $\rho_{\mu\nu}(q) = \rho_s(q^2) \delta_{\mu\nu} + \rho_q(q^2) \not{q}_{\mu\nu}$  [33], where  $\rho_s$  and  $\rho_q$  are two scalar functions of  $q^2$ . Correspondingly, we have

$$\Pi_{\mu\nu}(q) = \Pi_s(q^2) \delta_{\mu\nu} + \Pi_q(q^2) \not{q}_{\mu\nu}, \quad (3)$$

where the coefficients are [33]

$$\Pi_j(q^2) = \int_0^\infty ds \frac{\rho_j(s)}{s - q^2} + \text{polynomials}, \quad j = s, q, \quad (4)$$

with  $s$  the threshold parameter ( $\sim M^2$  for a nucleon). For example, the simplest phenomenological nucleon spectral densities take the form  $\rho_s^{\text{phen}}(s) = M \delta(s - M^2)$  and  $\rho_q^{\text{phen}}(s) = \delta(s - M^2)$ , corresponding to  $\Pi(q) = -(\not{q} + M)/(q^2 - M^2 + i0^+)$ , which is the standard nucleon propagator in vacuum, i.e., the two-point nucleon-nucleon correlation function.

For two operators  $A$  and  $B$ , the OPE gives  $TA(x)B(0) = \sum_n C_n^{AB}(x, \mu) \mathcal{O}_n(0, \mu)$  as  $x \rightarrow 0$ , where  $C_n^{AB}$ 's are the Wilson's coefficients, which can be obtained by standard perturbative methods [43], and  $\mu$  is the renormalization energy scale. In the momentum space, we thus have  $\Pi_j(Q^2) = \sum_n C_n^j(Q^2) \langle \mathcal{O}_n \rangle$ , where  $Q^2 = -q^2$ , and  $\langle \mathcal{O}_n \rangle$ 's are different types of quark/gluon condensates [33]. We note that the OPE is only meaningful in the deep space-like region.

Furthermore, for any function of momentum transfer, the Borel transformation  $\mathcal{B}[f(Q^2)] \equiv \hat{f}(\mathcal{M}^2)$  is defined by [33]

$$\hat{f}(\mathcal{M}^2) \equiv \lim_{\substack{Q^2, n \rightarrow \infty \\ Q^2/n = \mathcal{M}^2}} \frac{(Q^2)^{n+1}}{n!} \left( -\frac{d}{dQ^2} \right)^n f(Q^2), \quad (5)$$

where  $\mathcal{M} \sim M$  is the Borel mass [42]. Under the Borel transformation, the correlation function Eq. (4) becomes

$$\hat{\Pi}_j(\mathcal{M}^2) = \int_0^\infty ds e^{-s/\mathcal{M}^2} \rho_j(s), \quad j = s, q, \quad (6)$$

where polynomials in Eq. (4) disappear.

After making the Borel transformation on the correlation functions both from the phenomenological side (i.e.,  $\Pi^{\text{phen}}$ , which encapsulates information of the spectral densities) and from the OPE ( $\Pi^{\text{OPE}}$ ) under some assumptions [33], we obtain the QCDSR equations apparently relating the nucleon self-energies and correspondingly the  $E_n(\rho)$  via Eq. (1) on the phenomenological side, and the quark/gluon condensates on the OPE side [30, 33, 38]. Physically, the correlation functions from OPE are not the same as those from the phenomenological side, and they may even be very different from each other. The basic assumption of QCDSR is that in some range of  $q^2$ , these different correlation functions are the same, in the sense that the physical quantities are insensitive to the Borel mass  $\mathcal{M}$  introduced [33]. This range of  $\mathcal{M}$  is often called the QCDSR window [33, 42].

It should be pointed out that QCDSR will become a little difficult as density/momentum increases for neutron matter problem. The spectral densities in nuclear medium are very complicated owing to the complicated medium effects (such as excitations and correlations), and only at low densities/momenta there exists a narrow resonance state (the  $\delta$ -peak) corresponding to the nucleon degree of freedom ( $\rho_s \sim M \delta(s - M^2) + \dots$  and  $\rho_q \sim \delta(s - M^2) + \dots$ ). As density/momentum increases, continuum excitations will eventually emerge and these high density/momentum states will have increasing importance at high densities/momenta. While on the other hand, in QCDSR, contributions from these poorly-known complicated high order states are suppressed by Borel transformation of the correlation functions (characterized by the factor  $e^{-s/\mathcal{M}^2}$ ), and they can be even removed (as the polynomials in Eq. (4)). As a rough estimate on the density region above which the QCDSR for nucleonic matter becomes broken down, we consider the formation of the  $\Delta$  resonance as an excited state in dense nucleonic matter. As shown in Ref. [44], the formation density of the first charged state of  $\Delta(1232)$  could be smaller than  $2\rho_0$ , even to be around the saturation density. Thus it is conservative to expect that the

QCDSR for nucleonic matter should not be applied at densities around or above  $2\rho_0$ . However, a comprehensive analysis of the applicable region of the conventional QCDSR for nucleonic matter deserve more further work.

At finite densities, a new term proportional to the nucleon velocity, i.e.,  $\Pi_u(q^2, qu)\not{u}_{\mu\nu}$  with  $qu = q_\mu u^\mu$  [33], should be added to Eq. (3). Similarly, the correlation functions constructed from quark/gluon condensates are then given by

$$\Pi_j(q^2, qu) = \sum_n C_n^j(q^2, qu) \langle \mathcal{O}_n \rangle_\rho, \quad (7)$$

where  $\langle \mathcal{O}_n \rangle_\rho$  are the condensates at finite densities [32, 33].

In this work, the quark/gluon condensates at finite densities up to mass dimension-6 are included in the QCDSR equations, i.e.,  $\langle \bar{q}q \rangle$ ,  $\langle (\alpha_s/\pi)G^2 \rangle$ ,  $\langle g_s \bar{q} \sigma \mathcal{G} q \rangle$ ,  $\langle g_s q^\dagger \sigma \mathcal{G} q \rangle$ ,  $\langle \bar{q} \Gamma_1 q \bar{q} \Gamma_2 q \rangle$  and  $\langle \bar{q} \Gamma_1 \lambda^A q \bar{q} \Gamma_2 \lambda^A q \rangle$ , see Refs. [36, 38] for more details. For the very relevance for the discussion in this paper, we write down the expression for the quark condensates, i.e.,

$$\langle \bar{q}q \rangle_{\rho, \delta} \approx \langle \bar{q}q \rangle_{\text{vac}} + \frac{\sigma_N}{2m_q} (1 \mp \xi \delta) \rho + \Phi (1 \mp g \delta) \rho^2, \quad (8)$$

where “−” (“+”) is for the u (d) quark,  $\delta = (\rho_n - \rho_p)/(\rho_n + \rho_p)$  is the isospin asymmetry of neutrons and protons in asymmetric nucleonic matter (ANM) with  $\rho_{n/p}$  the neutron/proton density. The corresponding condensate in vacuum takes  $\langle \bar{q}q \rangle_{\text{vac}} \approx -(252 \text{ MeV})^3$  [33]. Moreover,  $\xi \approx 0.1$  characterizing the density dependence of the condensates for different quarks is fixed by the mass relation of the baryon octet [36],  $m_q \equiv (m_u + m_d)/2 \approx 3.5 \text{ MeV}$  is the average mass of two light quarks, and  $\sigma_N \equiv m_q dM/dm_q \approx 45 \text{ MeV}$  is the pion-nucleon sigma term [45].

The motivation of including the last term “ $\Phi(1 \mp g\delta)\rho^2$ ” in Eq. (8) is as follows: As the density increases, the linear density approximation for the chiral condensates becomes worse eventually, and high order terms in density should be included in the  $\langle \bar{q}q \rangle_{\rho, \delta}$ . However, the density dependence of the chiral condensates is extremely complicated, and there is no general power counting scheme to incorporate these high density terms. Besides the  $\rho^2$  term we adopted here, for instance, based on the chiral effective theories [22, 46], a term proportional to  $\rho^{5/3}$  was found in the perturbative expansion of  $\langle \bar{q}q \rangle_{\rho, \delta}$  in  $\rho$ . On the other hand, using the chiral Ward identity [47], a  $\rho^{4/3}$  term was found in the density expansion in the chiral condensates. In our work, including the higher-order  $\rho^2$  term is mainly for the improvement of describing the empirical EOS of PNM around and above saturation density, for which we use the celebrated Akmal–Pandharipande–Ravenhall (APR) EOS [48]. In this sense, the  $\Phi$ -term we adopted here is an effective correction to the chiral condensates beyond the linear leading-order. Two aspects related to the  $\Phi$ -term should be pointed out: 1). Without the higher-order  $\rho^2$  term, the EOS of PNM around and above saturation density can not be adjusted to be consistent with that of APR EOS, i.e., there exists systematic discrepancy between the QCDSR EOS and the APR EOS around and above saturation density; 2). Using an effective correction with a different power in density, e.g., a  $\rho^{5/3}$  term, the conclusion does

not change, i.e., the EOS of PNM around and above saturation density can still be adjusted to fit the APR EOS, and the sign of the coefficients  $\Phi$  and  $g$  does not change, and this will be seen from Fig. 1 in the following. Moreover, the physical origin of the high density term in the chiral condensates is an interesting issue, and one of the possibilities is the three-body force. For instance, in the Skyrme–Hartree–Fock (SHF) model, a traditional two-body force contributes a term proportional to  $\rho$  to the EOS, and a  $\rho^{1+\alpha}$  term emerges once the effective three-body force is considered [49]. Here  $\alpha$  is a parameter characterizing the three-body force. Exploring the three-body force in the QCDSR [35] and its connection to the high density term in the chiral condensates will be useful for further applications of the QCDSR in nucleonic matter calculations. In the following, we abbreviate the QCDSR using the chiral condensate without the last term in Eq. (8) in “naive QCDSR”.

Furthermore, the four-quark condensate used in this work takes the conventional decomposition structure as

$$\widetilde{\langle \bar{q}q \rangle^2}_{\rho, \delta} = (1 - f) \langle \bar{q}q \rangle_{\text{vac}}^2 + f \langle \bar{q}q \rangle_{\rho, \delta}^2, \quad (9)$$

where  $f$  is an effective parameter introduced in Refs. [32, 33, 36]. Besides the above input on the chiral/conventional four-quark condensates, the other condensates are adopted as the same as those in Refs. [32, 33, 36]. Effects of twist-four four-quark condensates [36] on the  $E_n(\rho)$  are not considered and will be discussed at the end of the next section. Finally, in carrying out the QCDSR calculations, we fix the central value of the  $E_n(\rho)$  at a very low density  $\rho_{v1} = 0.02 \text{ fm}^{-3}$  to be consistent with the prediction by the chiral perturbative theories (ChPT) [20, 21], i.e.,  $E_n(\rho_{v1}) = 4.2 \text{ MeV}$ , the central value of the symmetry energy  $E_{\text{sym}}(\rho)$  at a critical density  $\rho_c = 0.11 \text{ fm}^{-3}$  to be  $E_{\text{sym}}(\rho_c) = 26.65 \text{ MeV}$  [50], and fit the EOS of PNM to the APR EOS, via varying  $\Phi$ ,  $g$  and  $f$ . We note that the parameter  $f$  is essentially determined by  $E_n(\rho_{v1})$ , and the overall fitting of the EOS of PNM to the APR EOS and the symmetry energy at  $\rho_c$  determines the other two parameters  $\Phi$  and  $g$ .

### III. EOS OF PNM FROM QCDSR

In Fig. 1, we show the predictions on the  $E_n(\rho)$  by QCDSR with  $\langle \bar{q}q \rangle_{\text{vac}} = -(252 \text{ MeV})^3$ ,  $\xi = 0.1$ ,  $m_q = 3.5 \text{ MeV}$ ,  $\sigma_N = 45 \text{ MeV}$ ,  $\Phi' \equiv \Phi \times \langle \bar{q}q \rangle_{\text{vac}} = 3.45$ ,  $g = -0.64$  and  $f = 0.43$ . In the case of the naive QCDSR, we fix  $E_n(\rho_{v1}) = 4.2 \text{ MeV}$  via varying the  $f$  parameter, and find  $f = 0.50$ . Also included in Fig. 1 are the results from ChPT [20, 21] (green band), quantum Monte Carlo (QMC) simulations combined with chiral force to next-to-next-to-leading order ( $N^2\text{LO}$ ) with [51] (blue band) and without [52] (magenta band) leading-order chiral three-nucleon interactions forces, next-to-leading order (NLO) lattice calculation [53] (magenta circle), and QMC simulations for PNM at very low densities [54] (green diamond). The result from analyzing experimental data on the electric dipole polarizability  $\alpha_D$  in  $^{208}\text{Pb}$  [17] is also shown for comparison. Based on the obtained  $\Phi$  and  $g$ , we can esti-



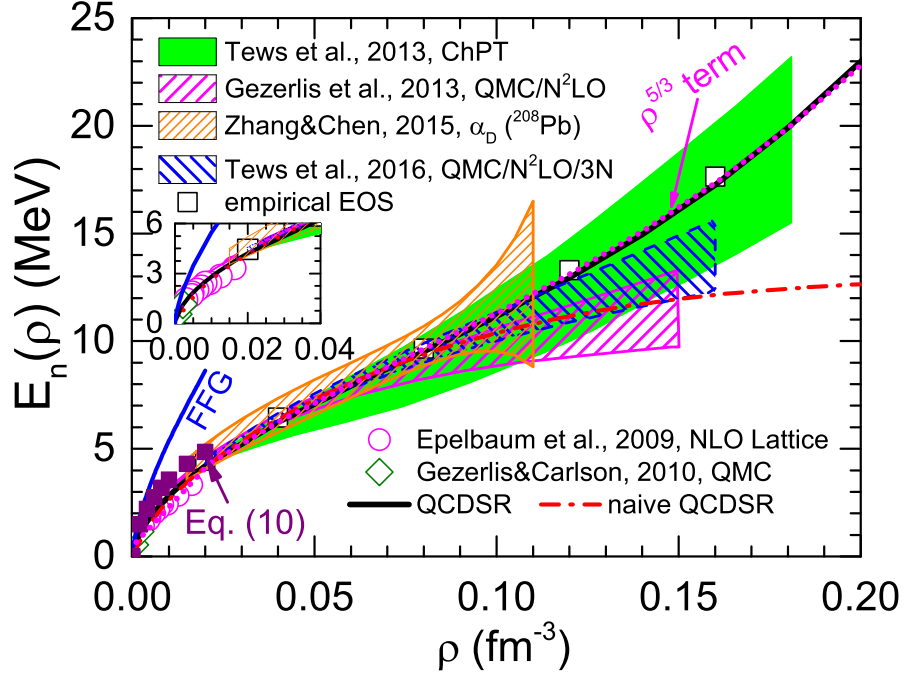


FIG. 1: (Color Online). EOS of PNMs obtained by QCD SR and by the naive QCD SR. Results from other approaches are also shown for comparison (see the text for details).

mate the density below which the  $\Phi$ -term has minor contribution to the quark condensates. This density can be estimated from  $|\Phi(1-g)\rho^2| \ll |(\sigma_N/2m_q)(1-\xi)\rho|$ , i.e., the last term in Eq. (8) is significantly less than the second term in Eq. (8), and we thus obtain  $\rho \ll \rho_{es} \approx 2.13 \text{ fm}^{-3}$ . Therefore, the effects of  $\Phi$  and  $g$  on the  $E_n(\rho)$  are trivial at subsaturation densities, e.g., when one artificially takes  $\Phi' = 0$  and keeping  $f$  fixed, the  $E_n(\rho_{vi})$  ( $E_n(0.1 \text{ fm}^{-3})$ ) changes from 4.20 MeV to 4.22 MeV (from 11.15 MeV to 10.01 MeV). It is thus reasonable to expect that effects of  $\Phi$  and  $g$  on the  $E_n(\rho)$  at low densities  $\lesssim 0.1 \text{ fm}^{-3}$  are small. However, as the density increases, there is no guarantee that the  $\Phi$ -term still has small effects on the EOS of PNMs since the  $E_n(\rho)$  is obtained by integrating over the density (see Eq. (1)).

The inset in Fig. 1 shows the EOS of PNMs at very low densities where the results are almost the same for the QCD SR and the naive QCD SR. Actually, after neglecting the contributions from dimension-4 and higher order terms, we can obtain an analytical approximation for EOS of PNMs as [38],

$$E_n(\rho) \approx E_n^{\text{FFG}}(\rho) - \frac{\rho}{2} \frac{M}{\langle \bar{q}q \rangle_{\text{vac}}} \left( 5 - \frac{\sigma_N}{2m_q} + \frac{\xi \sigma_N}{2m_q} \right), \quad (10)$$

where  $E_n^{\text{FFG}}(\rho) = 3k_F^{n,2}/10M \sim \rho^{2/3}$  is the free Fermi gas (FFG) prediction. Eq. (10) clearly demonstrates how the chiral condensate goes into play in the EOS of PNMs, i.e., the second term characterized by several constants ( $\xi$ ,  $\sigma_N$ ,  $m_q$  and  $\langle \bar{q}q \rangle_{\text{vac}}$ ) is negative, leading to a reduction on the  $E_n(\rho)$  compared to the FFG prediction. In Fig. 1, we also plot the results obtained from Eq. (10) at densities  $\lesssim 0.02 \text{ fm}^{-3}$  (violet solid square). One can see that the approximation Eq. (10)

can already produce reasonably the  $E_n(\rho)$  at low densities. Furthermore, it is seen from Fig. 1 that the prediction on the  $E_n(\rho)$  from QCD SR is consistent with several QMC simulations and lattice computation, showing QCD SR is a reliable approach in the study of PNMs, especially at lower densities, where the naive QCD SR is good enough.

Another feature of Fig. 1 is that compared with the APR EOS, the prediction on the EOS of PNMs in the naive QCD SR is well-behaved for  $\rho \lesssim 0.1 \text{ fm}^{-3}$ . However, as the density increases, the discrepancy between the overall shape of  $E_n(\rho)$  predicted by the naive QCD SR and by the APR becomes large and this can not be improved by adjusting the parameter  $f$  in the naive QCD SR, indicating that the leading-order linear density approximation for the chiral condensates does not work well enough and the higher order density terms in the chiral condensates are needed for PNMs calculations in the density region of  $\rho \gtrsim 0.1 \text{ fm}^{-3}$ . Once we consider the term  $\Phi g \rho^2$  in Eq. (8) for PNMs, and recalculate the EOS of PNMs, we find that compared with the case of the naive QCD SR, the obtained prediction can be largely improved to fit the APR EOS. For example, the EOS of PNMs at  $0.12 \text{ fm}^{-3}$  is now found to be 12.9 MeV, which is very close to the APR prediction 13.3 MeV. This feature suggests that the QCD SR with effective higher order density terms in quark condensates can be used to study the EOS of dense nucleonic matter at higher densities. It is necessary to point out that using a different high density term in Eq. (8) and re-fix the parameters  $f$ ,  $\Phi$  and  $g$  by the same fitting scheme, the density behavior of the  $E_n(\rho)$  is almost unchanged. For instance, when adopting a  $\rho^{5/3}$  term, i.e.,  $\Phi(1 \mp g\delta)\rho^{5/3}$ , we then obtain  $f \approx 0.46$ ,  $\Phi' \equiv \Phi \times \langle \bar{q}q \rangle_{\text{vac}}^{2/3} \approx 1.61$  and  $g \approx -0.34$ , and the corre-

sponding  $E_n(\rho)$  is shown in Fig. 1 by the magenta dot line. It is clearly seen that using a different high density term in the chiral condensates will not change our conclusions on the EOS of PNM.

Furthermore, it should be noted that once the twist-four four-quark condensates [36] are included in the QCDSR equations and the  $E_n(\rho)$  is still fixed at  $0.02 \text{ fm}^{-3}$  and made to be consistent with the APR EOS as much as possible, we find that the EOS of PNM at densities  $\lesssim 0.12 \text{ fm}^{-3}$  is essentially the same as the one without these condensates. And at nuclear saturation density  $\rho_0 = 0.16 \text{ fm}^{-3}$ , the  $E_n(\rho_0)$  changes from about 17.1 MeV to 15.9 MeV. As the high-twist operators have some impacts on several processes in hadronic physics [55], the exact knowledge on density dependence of the EOS of PNM may provide a novel tool to study them. Since including the twist-four four-quark condensates does not affect our present conclusions, we will not discuss effects of these terms again in the following sections and leave the details to be reported elsewhere [38].

Finally, we would like to briefly discuss the properties of the EOS of symmetric nuclear matter (SNM) obtained in the QCDSR. Although our main point on the above fitting scheme is the EOS of PNM at densities of  $\rho \lesssim \rho_0$  and the symmetry energy at  $\rho_c$  with the inclusion of an effective correction in  $\rho^2$ , the predictions on the saturation properties of the SNM are significantly improved from  $(\rho_0, E_0(\rho_0)) \approx (0.6 \text{ fm}^{-3}, -99 \text{ MeV})$  in the naive QCDSR to  $(0.2 \text{ fm}^{-3}, -26 \text{ MeV})$  in the QCDSR. It suggests from another viewpoint that the effective  $\Phi$ -term in Eq. (8) is important, implying the breakdown of the chiral condensates at linear order at densities even smaller than the saturation density. In fact, it is a challenging problem on how to improve the saturation properties of the SNM in the microscopic theories (see, e.g., Ref. [56]). Improvement on the saturation properties of the SNM in the QCDSR is important, and this is beyond the main motivation of the present work.

#### IV. CHIRAL CONDENSATES

In Fig. 2, we show the density dependence of the quark condensates from QCDSR as well as the corresponding predictions from ChPT [22, 46, 57] and the functional renormalization group (FRG) approach [23]. At low densities, the chiral condensate is dominated by the linear density term. Specifically, we have  $(\langle \bar{u}u \rangle_\rho - \langle \bar{d}d \rangle_\rho) / \langle \bar{q}q \rangle_{\text{vac}} \approx -\rho \sigma_N \xi / m_q \langle \bar{q}q \rangle_{\text{vac}} > 0$  at low densities, since  $\langle \bar{q}q \rangle_{\text{vac}}$  is negative. As density increases, the  $\Phi$  term in Eq. (8) begins to dominate and even to flip the relative relation of the magnitude between  $\langle \bar{u}u \rangle_\rho$  and  $\langle \bar{d}d \rangle_\rho$ , leading to  $\langle \bar{u}u \rangle_\rho / \langle \bar{q}q \rangle_{\text{vac}} < \langle \bar{d}d \rangle_\rho / \langle \bar{q}q \rangle_{\text{vac}}$  when the density  $\rho$  is larger than about  $0.15 \text{ fm}^{-3}$ . For example,  $\langle \bar{d}d \rangle_{\rho_0} / \langle \bar{q}q \rangle_{\text{vac}}$  ( $\langle \bar{u}u \rangle_{\rho_0} / \langle \bar{q}q \rangle_{\text{vac}}$ ) in PNM changes from 0.45 (0.56) in the linear density approximation to 0.60 (0.59) with the inclusion of the  $\Phi$  term in Eq. (8), leading to an enhancement of about 33% (5%). It is interesting to point out that the flip is a direct consequence of the inclusion of the higher order  $\Phi$  term in Eq. (8).

Furthermore, it is interesting to see that the high order  $\Phi$

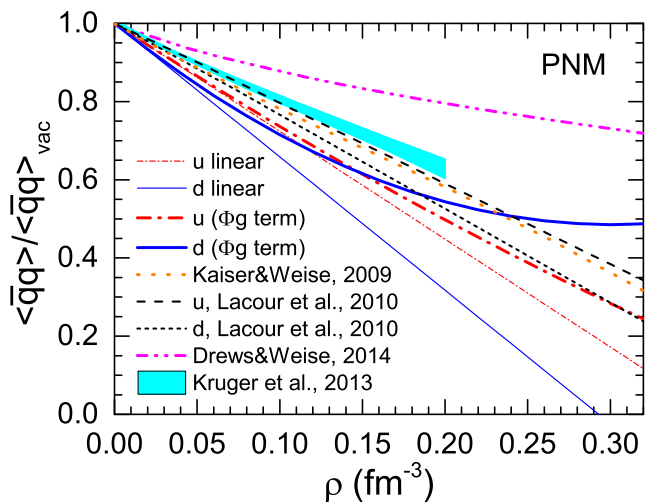


FIG. 2: (Color Online). Density dependence of quark condensates in PNM from QCDSR. Also shown are the results from ChPT [22, 46, 57] and FRG approach [23].

term in Eq. (8) tends to stabilize the chiral condensate both for u and d quarks at higher densities, while the leading-order linear density approximation Eq. (8) leads to chiral symmetry restoration at a density of about  $2\rho_0$ . This hindrance of the chiral symmetry restoration due to the high order density terms in quark condensates has important implications on the physical degrees of freedom in the core of neutron stars where the matter is very close to PNM. This feature is consistent with the recent analysis on the same issue using the FRG method [23].

At this point, we would like to discuss the role played by the  $\sigma_N$ . In our calculations above, the value of  $\sigma_N$  is fixed at 45 MeV. The physical value of  $\sigma_N$  still has a sizable uncertainty. With a different  $\sigma_N$ , however, we need to readjust the values of the parameters  $f$ ,  $\Phi$  and  $g$  based on the fitting scheme we adopted above, i.e., fixing the physical value of the EOS of PNM at  $\rho_{N1}$  and the symmetry energy at  $\rho_c$ , and meanwhile fitting the  $E_n(\rho)$  to the APR EOS. Consequently, in this way, the  $\sigma_N$  has very little influence on the EOS of PNM. Different values of  $\sigma_N$  will lead to different values of  $\Phi$  and  $g$ , but the density dependence of the chiral condensates will change only quantitatively, instead of qualitatively since the  $\sigma_N$  term (linear order) is a perturbation to the vacuum chiral condensates. Similarly, the  $\Phi$ -term is a perturbation to the linear term. Besides the quantities involved in the fitting scheme, the  $\sigma_N$  will also have influence on some other quantities such as the density dependence of the nucleon effective mass, which will be explored in detail elsewhere [38]. Finally, it should be mentioned that the study on the  $\sigma_N$  itself is an important issue, and it will help improving our understanding on the relevant aspects of the strong interaction.

## V. SUMMARY

We have studied the EOS of PNM  $E_n(\rho)$  within the framework of QCDSR by effectively taking into account the higher-order density effects in the quark condensates. Firstly, the  $E_n(\rho)$  thus obtained is found to be consistent with the predictions from current advanced microscopic many-body theories. Our results have indicated that although the higher-order density terms in quark condensates play minor role for EOS of PNM at subsaturation densities ( $\rho \lesssim 0.1 \text{ fm}^{-3}$ ), they play an important role in describing the EOS of PNM in the density region around and above nuclear saturation density.

Secondly, our results have demonstrated that the higher-order density terms in quark condensates tends to stabilize the u/d chiral condensates at higher densities, which is consistent with the predictions from other advanced microscopic many-body calculations. This feature has important implications on

the QCD phase diagram under extreme conditions of low temperatures, large isospin and large baryon chemical potentials, which is essential for understanding the physical degrees of freedom in the core of neutron stars.

## Acknowledgments

This work was supported in part by the National Natural Science Foundation of China under Grant No. 11625521, the Major State Basic Research Development Program (973 Program) in China under Contract No. 2015CB856904, the Program for Professor of Special Appointment (Eastern Scholar) at Shanghai Institutions of Higher Learning, Key Laboratory for Particle Physics, Astrophysics and Cosmology, Ministry of Education, China, and the Science and Technology Commission of Shanghai Municipality (11DZ2260700).

- 
- [1] S.N. Tan, *Ann. Phys.* **323**, 2952 (2008); **323**, 2971 (2008); **323**, 2987 (2008).
- [2] B.J. Cai and B.A. Li, *Phys. Rev. C* **92**, 011601(R) (2015).
- [3] T. Krüger, K. Hebeler, and A. Schwenk, *Phys. Lett.* **B744**, 18 (2015).
- [4] E.E. Kolomeitsev, J.M. Lattimer, A. Ohnishi, and I. Tews, arXiv:1611.07133.
- [5] N.B. Zhang, B.J. Cai, B.A. Li, W.G. Newton, and J. Xu, *Nucl. Sci. Tech.* **28**, 181 (2017).
- [6] O. Hen *et al.*, *Science* **346**, 614 (2014).
- [7] O. Hen, L.B. Weinstein, E. Piasetzky, G.A. Miller, M. Sargsian, and Y. Sagi, *Phys. Rev. C* **92**, 045205 (2015).
- [8] S. Giorgini, L.P. Pitaevskii, and S. Stringari, *Rev. Mod. Phys.* **85**, 1225 (2008).
- [9] I. Bloch, J. Dalibard, and W. Zwerger, *Rev. Mod. Phys.* **80**, 885 (2008).
- [10] W. Zwerger, ed., *The BCS-BEC Crossover and the Unitary Fermi Gas*, Lecture Notes in Physics, Springer, 2012.
- [11] N.K. Glendenning, *Compact Stars*, 2nd edition, Springer-Verlag New York, Inc., 2000.
- [12] J.M. Lattimer and M. Prakash, *Science* **304**, 536 (2004); *Phys. Rep.* **442**, 109 (2007).
- [13] J.M. Lattimer, *Annu. Rev. Nucl. Part. Sci.* **62**, 485 (2012).
- [14] F. Özel and P. Freire, *Ann. Rev. Astronomy and Astrophysics*, **54**, 401 (2016).
- [15] B.A. Li, A. Ramos, G. Verde, and I. Vidaña, eds., “*Topical issue on nuclear symmetry energy*”, *Eur. Phys. J. A* **50**, No. 2 (2014).
- [16] P. Haensel, A.Y. Potekhin, and D.G. Yakovlev, *Neutron Stars I*, Springer, 2007.
- [17] Z. Zhang and L.W. Chen, *Phys. Rev. C* **92**, 031301(R) (2015).
- [18] J.R. Stone and P.G. Reinhard, *Prog. Nucl. Part. Phys.* **58**, 587 (2006).
- [19] B.D. Serot and J.D. Walecka, *Adv. Nucl. Phys.* **16**, 1 (1986).
- [20] I. Tews, T. Krüger, K. Hebeler, and A. Schwenk, *Phys. Rev. Lett.* **110**, 032504 (2013).
- [21] T. Krüger, I. Tews, K. Hebeler, and A. Schwenk, *Phys. Rev. C* **88**, 025802 (2013).
- [22] T. Krüger, I. Tews, B. Friman, K. Hebeler, and A. Schwenk, *Phys. Lett.* **B726**, 412 (2013).
- [23] M. Drews and W. Weise, *Phys. Lett.* **B738**, 187 (2014).
- [24] G. Hagen, T. Papenbrock, A. Ekström, K. A. Wendt, G. Baard-  
sen, S. Gandolfi, M. Hjorth-Jensen, and C. J. Horowitz, *Phys. Rev. C* **89**, 014319 (2014).
- [25] K. Hebeler, J.D. Holt, J. Menendez, and A. Schwenk, *Annu. Rev. Nucl. Part. Sci.* **65**, 457 (2015).
- [26] C. Drischler, A. Carbone, K. Hebeler, and A. Schwenk, *Phys. Rev. C* **94**, 054307 (2016).
- [27] J. Carlson *et al.*, *Rev. Mod. Phys.* **87**, 1067 (2015).
- [28] M.A. Shifman, A.I. Vainshtein, and V.I. Zakharov, *Nucl. Phys.* **B147**, 385 (1979); **B147**, 448 (1979); **B147**, 519 (1979).
- [29] E.G. Drukarev and E.M. Levin, *Nucl. Phys.* **A511**, 679 (1990); **A516**, 715(E) (1990); *Prog. Part. Nucl. Phys.* **27**, 77 (1991).
- [30] T.D. Cohen, R.J. Furnstahl, and D.K. Griegel, *Phys. Rev. Lett.* **67**, 961 (1991); *Phys. Rev. C* **45**, 1881 (1992).
- [31] R.J. Furnstahl, D.K. Griegel, and T.D. Cohen, *Phys. Rev. C* **46**, 1507 (1992).
- [32] X.M. Jin, T.D. Cohen, R.J. Furnstahl, and D.K. Griegel, *Phys. Rev. C* **47**, 2882 (1993); *Phys. Rev. C* **49**, 464 (1994).
- [33] T.D. Cohen, R.J. Furnstahl, D.K. Griegel, and X.M. Jin, *Prog. Part. Nucl. Phys.* **35**, 221 (1995).
- [34] E.G. Drukarev, M.G. Ryskin, and V.A. Sadovnikova, *Phys. Rev. C* **70**, 065206 (2004); *Phys. Atom. Nucl.* **75**, 334 (2012).
- [35] E. G. Drukarev, M. G. Ryskin, and V. A. Sadovnikova, *Nucl. Phys.* **A959**, 129 (2017); *Nucl. Phys.* **A968**, 350 (2017).
- [36] K.S. Jeong and S.H. Lee, *Phys. Rev. C* **87**, 015204 (2013); *Eur. Phys. J. A* **50**, 16 (2014).
- [37] B.L. Ioffe, V.S. Fadin, and L.N. Lipatov, *Quantum Chromodynamics, Perturbative and Nonperturbative Aspects*, Cambridge, 2011, Chap. 6.
- [38] B.J. Cai and L.W. Chen, manuscript in preparation (2018).
- [39] G.F. Bertsch and S.D. Gupta, *Phys. Rep.* **160**, 189 (1988).
- [40] C. Xu, B.A. Li, L.W. Chen, and C.M. Ko, *Nucl. Phys.* **A865**, 1 (2011).
- [41] B.J. Cai and L.W. Chen, *Phys. Lett.* **B711**, 104 (2012).
- [42] B.L. Ioffe, *Nucl. Phys.* **B188**, 317 (1981).
- [43] K. Wilson, *Phys. Rev.* **179**, 1499 (1969).
- [44] B.J. Cai, F.J. Fattoyev, B.A. Li, and W.G. Newton, *Phys. Rev. C* **92**, 015802 (2015).
- [45] J. Gasser, H. Leutwyler, and M.E. Sainio, *Phys. Lett.* **B253**, 252 (1991).
- [46] N. Kaiser and W. Weise, *Phys. Lett.* **B671**, 25 (2009).
- [47] S. Goda and D. Jido, *Phys. Rev. C* **88**, 065204 (2013).

- [48] A. Akmal, V.R. Pandharipande, and D.G. Ravenhall, Phys. Rev. C **58**, 1804 (1998).
- [49] Z. Zhang and L.W. Chen, Phys. Rev. C **94**, 064326 (2016).
- [50] Z. Zhang and L.W. Chen, Phys. Lett. **B726**, 234 (2013).
- [51] I. Tews, S. Gandolfi, A. Gezerlis, and A. Schwenk, Phys. Rev. C **93**, 024305 (2016).
- [52] A. Gezerlis, I. Tews, E. Epelbaum, S. Gandolfi, K. Hebeler, A. Nogga, and A. Schwenk, Phys. Rev. Lett. **111**, 032501 (2013).
- [53] E. Epelbaum, H. Krebs, D. Lee, and Ulf-G. Meissner, Eur. Phys. A **40**, 199 (2009).
- [54] A. Gezerlis and J. Carlson, Phys. Rev. C **81**, 025803 (2010).
- [55] W. Greiner, S. Schramm, and E. Stein, *Quantum Chromodynamics*, Springer, 2007.
- [56] C. Drischler, K. Hebeler, and A. Schwenk, arXiv: 1710.08220.
- [57] A. Lacour, J.A. Oller, and Ulf-G. Meissner, J. Phys. G **37**, 125002 (2010).